Broecker, Eds. (NATO ASI series, Springer-Verlag, Berlin/Heidelberg, Germany, 1992), pp. 141–153.
29. L. R. McHargue, P. E. Damon, D. J. Donahue, *Geophys. Res. Lett.* **22**, 659 (1995).
30. G. C. Castagnoli *et al.*, *ibid.*, p. 707.
31. J. C. Vogel, *Radiocarbon* **25**, 213 (1983).
32. H. Oeschger, in *Nuclear and Chemical Dating Techniques: Interpreting the Environmental Record*, L. A. Currie, Ed. (American Chemical Society, Washington, DC, 1982), pp. 5–42.
33. G. M. Raisbeck *et al.*, in (*28*), pp. 127–139.
34. C. P. Sonnett *et al.*, *Nature* **330,** 458 (1987).
35. J. C. Liddicoat *et al.*, *Geophys. J. Int*. **108**, 422 (1992); P. Vlag *et al.*, *J. Geophys. Res*. **101**, 28211 (1996).
36. J. C. Vogel and J. Kronfeld, *Radiocarbon* **39**, 27 (1997).
37. F. Yiou, *et al.*, *J. Geophys. Res*. **102**, 26783 (1997); R.C. Finkel and K. Nishiizumi, *ibid.*, p. 26699.
38. We thank the Lake Suigetsu Scientific Drilling Team led by Y. Yasuda; M Nishimura for the macrofossils collection from sediments; and E. R. M. Druffel and three anonymous reviewers for comments on the manuscript. This work was funded primarily by the Grant-Aid for Scientific Research (04214116) from the Ministry of Education, Science, and Culture (Japan) and partly by the Toyota Foundation (96-A-232).

1 October 1997; accepted 20 January 1998

Probing Single Secretory Vesicles with Capillary Electrophoresis

Daniel T. Chiu, Sheri J. Lillard, Richard H. Scheller, Richard N. Zare,* Sandra E. Rodriguez-Cruz, Evan R. Williams, Owe Orwar, Mats Sandberg, J. Anders Lundqvist

Secretory vesicles obtained from the atrial gland of the gastropod mollusk *Aplysia californica* were chemically analyzed individually with a combination of optical trapping, capillary electrophoresis separation, and a laser-induced fluorescence detection. With the use of optical trapping, a single vesicle that had attoliters (10^{-18} liters) of volume was introduced into the tapered inlet of a separation capillary. Once the vesicle was injected, it was lysed, and its components were fluorescently labeled with naphthalene-2,3-dicarboxaldehyde before separation. The resultant electropherograms indicated distinct variations in the contents of single vesicles.

Biological messengers are synthesized intracellularly and packaged into secretory vesicles, where they are stored until a physiological signal triggers fusion of the vesicle membrane with the plasma membrane, resulting in the extracellular release of a chemical messenger. This mode of cellular signaling is used by all eukaryotic organisms in biological processes ranging from sensory perception to the regulation of reproductive cycles. Analysis of secretory products has been done on populations of vesicles, but the contents of a single vesicle are often sufficient to produce a biological response. Therefore, it is important to develop techniques of adequate sensitivity to characterize the array of chemical messengers within individual vesicles (*1*, *2*). The sizes of vesicles range from 30 to 2000 nm, which corresponds to volumes from zeptoliters (10^{-21} liters) to low femtoliters (10^{-15} liters), respectively. The minute size of secretory vesicles makes their study by traditional analytical methods impossible.

D. T. Chiu, S. J. Lillard, R. N. Zare, Department of Chemistry, Stanford University, Stanford, CA 94305, USA.
R. H. Scheller, Department of Molecular and Cellular Physiology, Howard Hughes Medical Institute, Stanford University, Stanford, CA 94305, USA.
S. E. Rodriguez-Cruz and E. R. Williams, Department of Chemistry, University of California, Berkeley, CA 94720, USA.
O. Orwar and J. A. Lundqvist, Department of Chemistry, Göteborg University, SE-412 96, Göteborg, Sweden.
M. Sandberg, Department of Anatomy and Cell Biology, Göteborg University, SE-413 90, Göteborg, Sweden.

*To whom correspondence should be addressed.

Recently, capillary electrophoresis (CE) has emerged as a powerful separation technique for the analysis of ultrasmall sample volumes (*3*). A much pursued goal in the area of ultrasensitive chemical analysis is the use of CE to separate and analyze the contents of single biological vesicles (*2*). Using such methods, one can compare the contents of single secretory vesicles one at a time, revealing variations that would otherwise be buried within the analysis of populations. This type of study provides insight into the cellular mechanisms used to package and sort chemical messengers into vesicles and defines sets of secreted bioactive products with a precision previously unattainable.

Two considerations in the use of CE for the analysis of single vesicles are detection sensitivity (*4*) and sample introduction (*5*, *6*). The sensitivity required to detect the laser-induced fluorescence (LIF) of a single dye molecule exists (*4*). Detection, however, is only the back half of the problem. Sample introduction and manipulation remain the primary challenge. Thus far, the analysis of single vesicles has been hindered by the difficulty of introducing a single vesicle into the separation capillary and analyzing its contents. Recently, the first part of this problem was overcome by the use of optical trapping and tapered capillaries (*5*). The second challenge is to label the contents of a single vesicle with a fluorophore for subsequent detection by LIF. In the present experiment, a miniature on-column derivatization scheme was applied to the molecules under investigation. The key to ensure an efficient on-column reaction is to minimize the reaction volume, which leads to a higher concentration of analyte molecules and a smaller number of labeling molecules. The technique of tapered capillaries (*5*) also addresses this challenge. For example, the on-column reaction volume for a normal capillary inlet with an inner diameter (i.d.) of 25 μm and a length of 1000 μm is 4.9×10^{-10} liters. The reaction volume for a tapered capillary inlet of 1-μm i.d. of the same length, however, is 7.8×10^{-13} liters. This reduction in volume by a factor of 625 leads to a faster and more efficient reaction with fewer unreacted dye molecules. With this manipulation capability and improved reaction conditions, the contents of single biological vesicles can be probed, one by one.

The vesicles studied in this experiment were obtained from the atrial gland of the gastropod mollusk *Aplysia californica* (*7*). These vesicles contain bioactive peptides

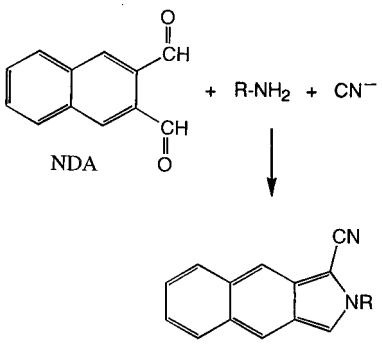

that are packaged into secretory granules called dense core vesicles (DCVs) (*8*). These DCVs are large (average diameter ≈ 1 μm) and can be easily isolated from *Aplysia*. This advantageous attribute of the DCVs has motivated their use in the present study. The atrial gland was first dissected from the distal end of the hermaphroditic duct, and subsequent slicing of the gland with a sharp razor blade released DCVs into a solution of artificial seawater. Most research on the atrial gland of *Aplysia* has been directed at the bioactive peptides (*9*), which are involved in this animal's reproductive behavior. Therefore, it is interesting to find in the present study that the DCVs also contain large amounts of primary amine-containing compounds of

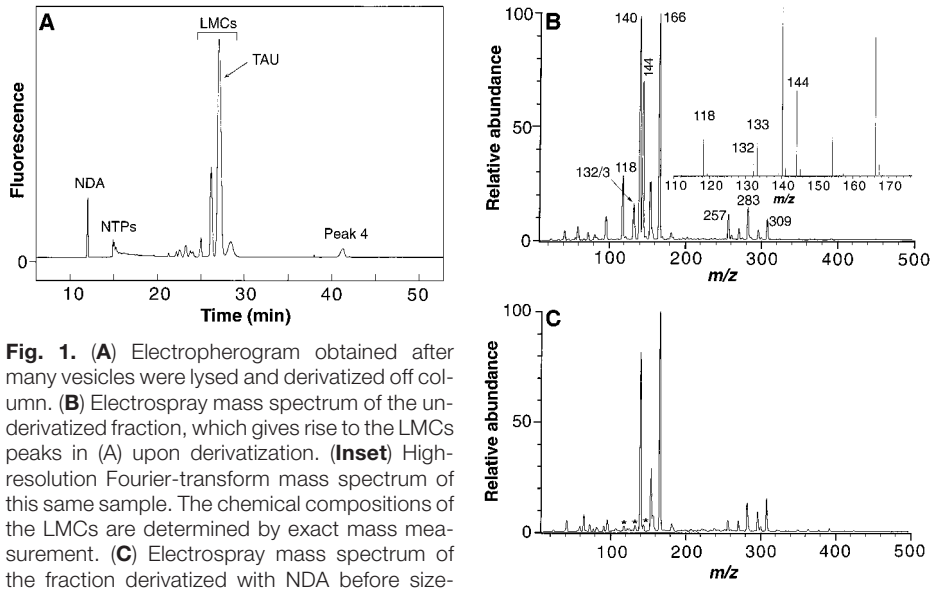

Fig. 1. (**A**) Electropherogram obtained after many vesicles were lysed and derivatized off column. (**B**) Electrospray mass spectrum of the underivatized fraction, which gives rise to the LMCs peaks in (A) upon derivatization. (**Inset**) High-resolution Fourier-transform mass spectrum of this same sample. The chemical compositions of the LMCs are determined by exact mass measurement. (**C**) Electrospray mass spectrum of the fraction derivatized with NDA before size-exclusion showing the disappearance of the peaks at *m/z* 118, 132/3, and 144.

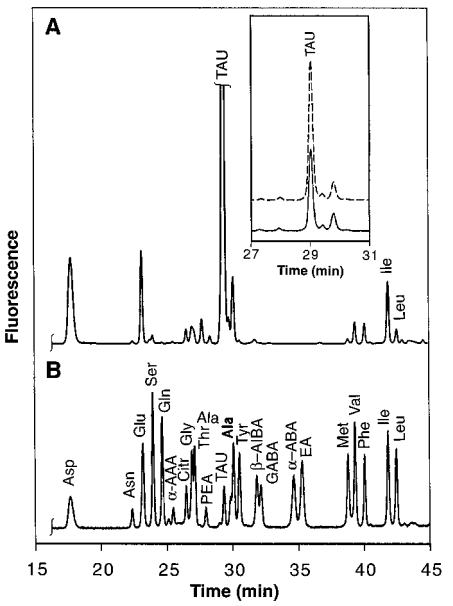

Fig. 2. (**A**) LC chromatogram of an OPA/βME–derivatized LMCs size-exclusion fraction. (**Inset**) Expanded view of the retention time of taurine before (solid trace) and after (dotted trace) the addition of taurine standards to the LMCs sample. Note the increase in the peak height of taurine (dotted trace). (**B**) LC chromatogram of a mixture of OPA/βME–derivatized amino acids standard. Abbreviations of nonstandard amino acids: α-AAA = α-aminoadipate, Citr = citrulline, PEA = phosphoethanolamine, TAU = taurine, β-AIBA = β-aminoisobutyrate, GABA = γ-aminobutyrate, α-ABA = α-aminobutyrate, and EA = ethanolamine.

low molecular weight.

Vesicles were lysed and then reacted off-column with naphthalene-2,3-dicarboxaldehyde (NDA) and potassium cyanide (KCN) (*10*). The NDA selectively reacts with primary amines in the presence of cyanide. The peaks detected in the electropherogram (*11*) (Fig. 1A) originate from NDA, NH_2-terminal peptides (NTPs) (*12*), low-mass compounds (LMCs) [of which taurine is the main component], and an unidentified peak (peak 4). The peak intensities suggest the LMCs are abundant. In addition to NTPs, the DCVs also contain high concentrations of Peptides A, B, and Califins (*9*). These peptides, however, were not identified by CE-LIF in the present study, probably because of their poor reaction efficiency with NDA.

We assigned the peak identified with NTPs by running synthesized and purified peptide standards. To characterize the LMCs peaks, we fractionated the contents of the vesicles by molecular weight through a size-exclusion column (*13*). The fraction containing the LMCs was identified by derivatization; the resulting fluorescent solution gave rise to the corresponding LMCs peaks in Fig. 1A. This fraction, both underivatized and derivatized before size exclusion, was analyzed by electrospray-ionization mass spectrometry (ESI-MS) (*14*–*16*) (Fig. 1, B and C, respectively). The abundances of the peaks present in the derivatized sample at mass-to-charge ratios (*m/z*) 118, 132.6, and 144 are insignificant compared with those in the underivatized sample. The depletion of these three peaks in Fig. 1C indicates that the LMCs reacted with NDA and KCN. No derivatized LMCs were observed in the ESI mass spectrum after derivatization of the solution in Fig. 1B, owing to poor electrospray efficiency of the NDA-derivatized LMCs. A high-resolution spectrum of the underivatized fraction, obtained with the use of an external electrospray ion-source Fourier-transform mass spectrometer (Fig. 1B, inset) (*17*), shows that the peak identified at low resolution as *m/z* 132.6 is actually composed of two unresolved peaks at *m/z* 132.103 and 133.135. All of the LMCs ions are formed by attachment of a single proton in the electrospray process. Therefore, the actual masses of the LMCs are determined to be *m/z* 117.079, 131.095, 132.127, and 143.094 (*18*). From these exact mass measurements, the chemical compositions of these compounds can be uniquely assigned as $C_5H_{11}NO_2$, $C_6H_{13}NO_2$, $C_6H_{16}N_2O$, and $C_7H_{13}NO_2$, respectively. By analyzing the LMCs samples with liquid chromatography (LC) and CE-LIF, we determined the identity of $C_6H_{13}NO_2$ to be leucine and isoleucine. The compounds $C_7H_{13}NO_2$ and $C_6H_{16}N_2O$ do not match the molecular mass of any common amino acids. Although the compound at mass 117.079 ($C_5H_{11}NO_2$) has the same chemical formula as valine, this peak does not match the fragmentation pattern of valine. It is possible that these peaks are derived from modified or unusual amino acids.

To further characterize the LMCs, we performed LC on size-exclusion fractions of atrial gland extracts derivatized with *o*-phthaldialdehyde/β-mercaptoethanol (OPA/βME) (*19*) (Fig. 2A). The reaction of OPA and a nucleophile such as βME with primary amines is similar to that of NDA and CN^-. Comparison of the retention times of known amino acid standards with those of the fractionated vesicle lysate show that the peak at ~29 min matches the retention time of taurine ($H_2NCH_2CH_2SO_3H$). Addition of taurine standard to this sample led to a corresponding increase in the height of this peak with excellent recovery (104%, n = 3) (Fig. 2A, inset, dotted trace). The identity of this peak as taurine was further confirmed by LC using a different mobile phase composition and was also indicated by ^1H nuclear magnetic resonance on isolated fractions. Because of the poor electrospray efficiency of taurine, it was not detected in the positive-ion ESI-MS spectra. The high intensity of the taurine peak in LC also suggests that it is the major amine-containing component. This finding was confirmed by CE-LIF using populations of vesicles with and without added taurine standards.

For analysis, the vesicle is first optically trapped (Fig. 3A), and the capillary tip is subsequently moved next to it (Fig. 3B). The vesicle is then electrokinetically introduced into the capillary with a small potential (Fig. 3C). Once the vesicle is injected, the capillary inlet is immediately transferred into a

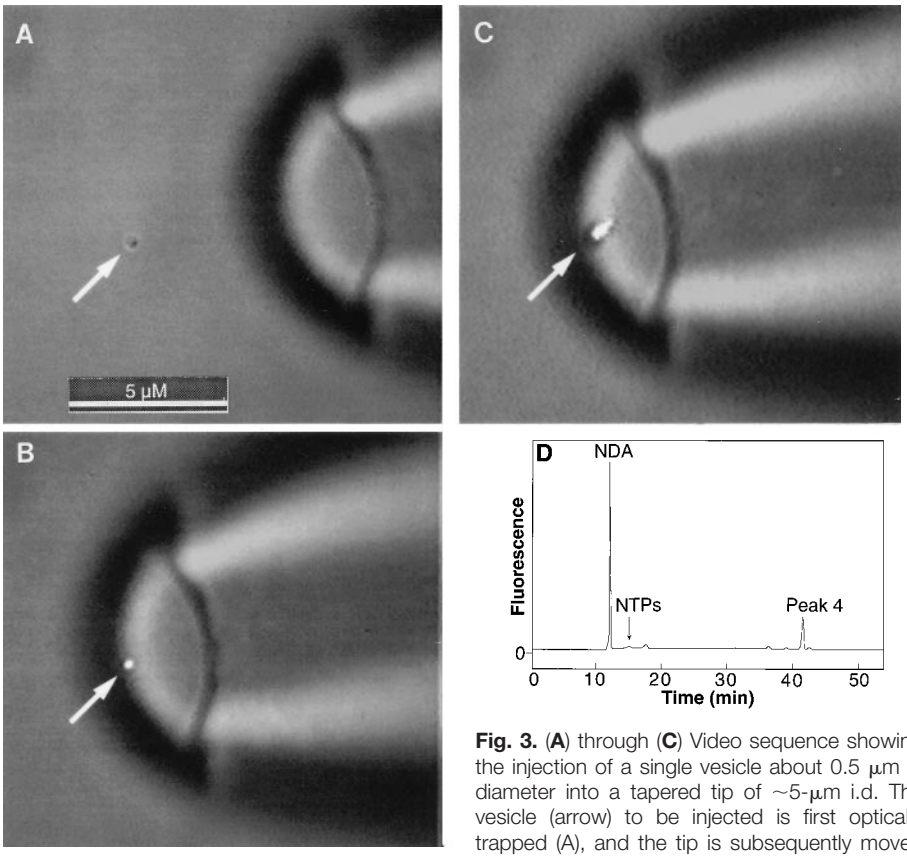

Fig. 3. (**A**) through (**C**) Video sequence showing the injection of a single vesicle about 0.5 μm in diameter into a tapered tip of ~5-μm i.d. The vesicle (arrow) to be injected is first optically trapped (A), and the tip is subsequently moved next to the vesicle (B). Upon application of a small voltage (C), the vesicle (arrow) is introduced electrokinetically into the tapered capillary inlet. Movement of the vesicle into the capillary causes the blurring observed in (C). (**D**) Electropherogram of the vesicle.

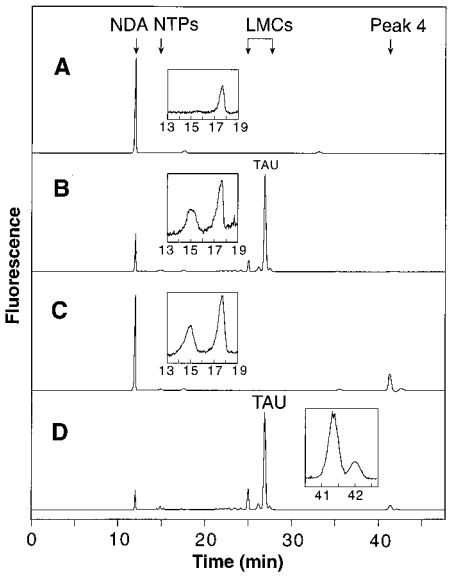

Fig. 4. (**A**) Control electropherogram in which no vesicles were injected. Electropherograms obtained from the injection of (**B**) and (**C**) single vesicles and (**D**) two vesicles. (**Insets**) Expanded views of the bracketed sections of the electropherograms.

small droplet of reaction mixture containing 1 mM NDA and 1 mM KCN in 10 mM borate buffer (10% acetonitrile). A small amount of this reaction mixture is electrokinetically injected into the tapered inlet to lyse the vesicle. The lysate is then permitted to react on column with NDA for 5 min at ambient temperature (20° to 25°C). After electrophoretic separation, the NDA-labeled components are detected with LIF. The resultant electropherogram (Fig. 3D) indicates that this vesicle contains NTPs and peak 4 but no taurine.

In control electropherograms (Fig. 4A), in which no vesicles were injected, the peak at ~12 min was caused by NDA. This peak was used as an internal standard for the normalization of migration times in all other electropherograms. Electropherograms obtained from two different single vesicles show that the contents of the vesicles are markedly different: one contains predominantly taurine but has no peak 4 (Fig. 4B), whereas the other is mainly composed of peak 4 with no taurine (Fig. 4C). Both also have NTPs (insets). From the 10 single vesicles that were analyzed, none contained taurine and peak 4 together. The amount of NTPs, however, remained approximately constant from vesicle to vesicle. When two vesicles were injected into the tapered capillary at the same time, the resulting electropherogram (Fig. 4D) revealed that both taurine and peak 4 were present, which indicates a mixing of the contents from two different types of vesicles, similar to what is found in a population analysis.

We have identified taurine as one of the most abundant molecules present in atrial gland vesicles. Taurine is physiologically active and is present in high concentrations in identified neurons of *A. californica* and in the central nervous system of mammals (*20*, *21*). Our observation of vesicular taurine demonstrates that the compound is stored and secreted, which strongly supports the proposed role of taurine as a neuromodulator or hormone. Taurine's presence in the atrial gland vesicles might also suggest a role in osmoregulation (*21*) or in the reproductive cycle of *Aplysia*. From the single-vesicle analysis, it is evident that the presence of taurine is accompanied by the lack of peak 4. This variation between single vesicles might be caused by two different populations of vesicles or by the same type of vesicles at different stages of maturity.

This technique, which can separate and probe the chemical messages contained in a single vesicle of only zepto- or attoliters of volume, should make it possible to address many previously unanswerable biological questions. Although the DCVs analyzed in this study are relatively large, their analysis marks the beginning of an era in which the information contained in a single vesicle can be probed and deciphered.

REFERENCES AND NOTES

1. K. Pihel *et al*. *Anal. Chem.* **67**, 4514 (1995).
2. S. J. Lillard, E. S. Yeung, M. A. McCloskey, *ibid.* **68**, 2897 (1996).
3. S. J. Lillard and E. S. Yeung, in *Handbook of Capillary Electrophoresis*, J. P. Landers, Ed. (CRC Press, Boca Raton, FL, 1996), pp. 523–544; J. A. Jankowski, S. Tracht, J. V. Sweedler, *Trends Anal. Chem.* **14**, 170 (1995); S. D. Gilman and A. G. Ewing, *Anal. Chem.* **67**, 58 (1995).
4. A. Castro and E. B. Shera, *Anal. Chem.* **67**, 3181 (1995).
5. D. T. Chiu *et al.*, *ibid.* **69**, 1801 (1997).
6. T. M. Olefirowicz and A. G. Ewing, *ibid.* **62**, 1872 (1990).
7. *Aplysia* are first anesthetized with an isotonic concentration of magnesium chloride, followed by dissection of the atrial gland and isolation of the vesicles.
8. W. S. Sossin, *et al.*, *J. Biol. Chem.* **264**, 16933 (1989).
9. R. J. Kaldany, J. R. Nambu, R. H. Scheller, *Annu. Rev. Neurosci.* **8**, 431 (1985); G. T. Nagle *et al.*, *J. Biol. Chem.* **263**, 9223 (1988).
10. P. de Montigny *et al.*, *Anal. Chem.* **59**, 1096 (1987); O. Orwar, H. A. Fishman, N. E. Ziv, R. H. Scheller, R. N. Zare, *ibid.* **67**, 4261 (1995).
11. All electropherograms were obtained with the use of a capillary with an inner diameter of 25 μm and an outer diameter of 150 μm. The separation buffer consisted of 75% 50 mM borate and 25% acetonitrile (pH = 9.0). The wavelength used to excite NDA fluorescence was either the 457.9-nm line of an argon ion laser or the 442-nm line of a HeCd laser.
12. W. R. A. van Heumen, G. T. Nagle, A. Kurosky,

Cell Tissue Res. **279**, 13 (1995).
13. The vesicle extract was run through a Bio-Rad Econo-Pac 10DG (Bio-Gel P-6DG) column, which has an exclusion limit of 6000 daltons and a fractionation range of 1000 to 6000 daltons.
14. J. B. Fenn *et al.*, *Science* **246**, 64 (1989).
15. The entire vesicle extract was electrosprayed into a Fourier-transform mass spectrometer. The two most abundant peaks were at *m/z* 144 and 118; ions corresponding to NTPs were observed in minor abundance.
16. Low-resolution ESI mass spectra were acquired on a home-built electrospray ionization quadrupole mass spectrometer, which is described in more detail in S. E. Rodriguez-Cruz, J. S. Klassen, E. R. Williams, *J. Am. Soc. Mass Spectrom.* **8**, 565 (1997).
17. E. R. Williams, *Trends Anal. Chem.* **13**, 247 (1994); D. S. Gross and E. R. Williams, *J. Am. Chem. Soc.* **117**, 883 (1995).
18. Exact masses were determined from four replicate measurements with a mass accuracy of better than 10 parts per million using internal calibration standards. Elemental compositions were assigned on the basis of the masses of the common elements and were constrained by the measured isotope distributions.
19. High-performance LC was run with a 25-cm-long column using two different mobile phase compositions (phosphate buffer at pH 5.40 and 6.50), with methanol as the organic modifier. Derivatization with *o*-phthalaldehyde/β-mercaptoethanol and reversed-phase LC was performed according to P. Lindroth and K. Mopper, *Anal. Chem.* **51**, 1667 (1979), with minor modifications [X. Li, A. Hallqvist, I. Jacobson, O. Orwar, M. Sandberg, *Brain Res.* **706**, 86 (1996)]. Detection was performed with the use of a deuterium light source (excitation: 330 nm; detection: 418 nm). Standard addition of taurine to the samples yielded high recoveries: 105% (pH = 5.40, n = 3) and 104% (pH = 6.50, n = 3).
20. R. McCaman and J. Stetzler, *J. Neurochem.* **29**, 739 (1977).
21. R. J. Huxtable, *Physiol. Rev.* **72**, 101 (1992).
22. We thank P. Schnier, R. Jockusch, and J. Klassen for technical assistance with mass spectrometry. We also thank G. T. Nagle and S. D. Painter for generously providing us with purified atrial gland peptides. S.J.L. acknowledges support from NIH for a postdoctoral fellowship (GM18386). O.O. is supported by the Swedish Natural Science Research Council (NFR) (10481-305, -308, and -309) and by the Swedish Foundation for Strategic Research (SSF). M.S. is supported by NFR (01-905-313). This work is supported by the International Joint Research Program (NEDO) of Japan, the U.S. National Institute on Drug Abuse (DA09873), NSF (CHE-9258178), and NIH (1R29GM50336-01A2).

17 September 1997; accepted 13 January 1998

Images of Interlayer Josephson Vortices in $Tl_2Ba_2CuO_{6+\delta}$

Kathryn A. Moler,* John R. Kirtley, D. G. Hinks, T. W. Li, Ming Xu†

The strength of the interlayer Josephson tunneling in layered superconductors is an essential test of the interlayer tunneling model as a mechanism for superconductivity, as well as a useful phenomenological parameter. A scanning superconducting quantum interference device (SQUID) microscope was used to image interlayer Josephson vortices in $Tl_2Ba_2CuO_{6+\delta}$ and to obtain a direct measure of the interlayer tunneling in a high–transition temperature superconductor with a single copper oxide plane per unit cell. The measured interlayer penetration depth, λ_c, is ~20 micrometers, about 20 times the penetration depth required by the interlayer tunneling model.

Although tremendous progress has been made over the past decade in understanding the phenomenological properties of the cuprate superconductors, in improving the quality of the materials, and in identifying the symmetry of the pairing state, the mechanism of the superconductivity remains unresolved. One candidate mechanism is the interlayer tunneling (ILT) model, in which the superconductivity results from an increased coupling between the layers in the superconducting state (*1*–*3*). For this model to succeed, the interlayer coupling in the superconducting state must be sufficiently strong to account for the large condensation energy of the cuprate superconductors (*3*–*5*). The best materials for testing this requirement are $Tl_2Ba_2CuO_{6+\delta}$ (Tl-2201) and $HgBa_2CuO_{4+\delta}$ (Hg-1201), which have high critical temperatures ($T_c \approx 90$ K) and a single copper oxide plane per unit cell.

The interlayer tunneling strength in cuprates is often inferred from the normal-state anisotropy, but a key point of the ILT model is that this correlation will be unconventional in the single-layer cuprates. It is therefore crucial to determine the interlayer coupling in the superconducting state. One measure of this coupling is the *c*-axis magnetic penetration depth, λ_c. Another measure is the Josephson plasma frequency (*6*, *7*), $\omega_p = c\lambda_c^{-1}\varepsilon^{-1/2}$, where ε is the dielectric constant of the interlayer medium and c is the speed of light. The Josephson resonance has not been detected in either Tl-2201 or Hg-1201. Van der Marel and colleagues reported an upper limit $\omega_p\,\varepsilon^{1/2} < 100$ cm^{-1} in Tl-2201 (*8*), a value difficult to explain within the ILT model (*4*). In contrast, recently measured magnetic susceptibility data on oriented powders of Hg-1201, analyzed with London's equation and assuming spherical grains, give $\lambda_c(T = 0) = 1.36 \pm 0.16$ μm for Hg-1201 (*9*), similar to the ILT value (*10*). Here, we used a SQUID microscope to image interlayer Josephson vortices in two single crystals of Tl-2201 and determine λ_c directly.

K. A. Moler, Department of Physics, Princeton University, Princeton, NJ 08544, USA.
J. R. Kirtley, IBM T. J. Watson Research Center, Post Office Box 218, Yorktown Heights, NY 10598, USA.
D. G. Hinks and T. W. Li, Materials Science Division, Argonne National Laboratory, Argonne, IL 60439, USA.
M. Xu, James Franck Institute, University of Chicago, Chicago, IL 60637, USA.

*To whom correspondence should be addressed.
†Present address: Lucent Technologies, 2000 North Naperville Road, Naperville, IL 60566, USA.

The phenomenological Lawrence-Doniach model for a stack of Josephson-coupled superconducting layers (*6*) is widely applied to highly anisotropic superconductors, including organics, cuprates, and artificially structured model systems. The structure of an isolated vortex parallel to the layers, or "interlayer Josephson vortex," is similar to a vortex in an anisotropic Ginzburg-Landau theory except at the vortex core (*11*). The spatial extent of the vortex along the layers, λ_c, is related to the critical current density between the layers, J_0, by

$$\lambda_c = (c\Phi_0/8\pi^2 s J_0)^{1/2} \qquad (1)$$

(*6*, *11*), where $\Phi_0 = hc/2e$ is the superconducting flux quantum, h is Planck's constant, e is the electron charge, and s is the interlayer spacing. A large vortex thus indicates a weak interlayer coupling.

In recent work, we used vortex imaging to directly measure the Josephson coupling across grain boundaries of $YBa_2Cu_3O_{7-\delta}$ (*12*) and the interlayer Josephson coupling in the quasi-two-dimensional (quasi-2D) organic superconductor κ-$(BEDT\text{-}TTF)_2Cu(NCS)_2$ (*13*). We now report the observation of isolated interlayer vortices in $Tl_2Ba_2CuO_{6+\delta}$. Although the *a*-axis penetration depth is substantially less than our spatial resolution of 8 μm, our images directly show the *c*-axis penetration depth $\lambda_c \approx 20$ μm.

Magnetic fields were imaged at the surface of the crystals with a scanning SQUID microscope (*14*). The SQUID is integrated with shielded leads to a square superconducting pickup loop (side length $L = 8.2$ μm) on the same chip. The SQUID detects the total magnetic flux through the pickup loop,

$$\Phi_s = \int_{\text{loop}} B_z(x, y, z = z_0)\,dx\,dy \qquad (2)$$

where B_z is the local magnetic field perpendicular to the sample surface, x and y are